# 5

# Slow Light in Optical Fibers

Shanglin Hou[1] and Wei Qiu[2]
[1]*School of Science, Lanzhou University of Technology, Lanzhou,*
[2]*Department of Physics, Liaoning University, Shenyang*
*China*

## 1. Introduction

The group velocity at which light pulses propagate through a dispersive material system is very different from the vacuum speed of light $c$, One refers to light as being "slow" for $v_g << c$ (Boyd & Gauthier, 2009) or "fast" for $v_g > c$ or $v_g < 0$ (Stenner et al, 2003 ). For $v_g < 0$, the pulse envelope appears to travel backward in the material (Gehring et al, 2006), and hence it is sometimes referred to as "backward light."

The subject of slow light has caused keen interest in the past decade or more, and it is possible to control the group velocity of light pulses in the dispersive materials. Interest in slow and fast light dates back to the early days of the 20th century. Sommerfeld and Brillouin (Sommerfeld & Brillouin, 1960) were intrigued by the fact that theory predicts that $v_g$ can exceed c, which leads to apparent inconsistencies with Einstein's special theory of relativity. Experimental investigations of extreme propagation velocities were performed soon after the invention of the laser (Faxvog and et al, 1970). In 1999, Harris's group research work greatly stimulated researchers' interests, which showed that light could be slowed down to 17m/s. The result was obtained in ultra cold atom clouds with the use of electromagnetically induced transparency (EIT), which induces transparency in a material while allowing it to retain strong linear and nonlinear optical properties (Hau et al, 1999). Slow light can also be obtained through the use of the optical response of hot atomic vapors (Philips et al, 2001). These early research works require hard conditions and the slow light cannot operate in room temperature.

Recently, researchers found ways to realize slow light operating in room temperature and solid-state materials, which are more suited for many practical applications, namely slow light via stimulated Brillouin scattering(SBS), slow light via coherent population oscillations (CPO), tunable time delays based on group velocity dispersion or conversion/ dispersion(C/D), slow light in fiber Bragg gratings and so on. In this chapter, we describe some of the physical mechanisms that can be used to induce slow and fast light effects in room-temperature solids (Bigelow et al, 2003) and some of the exotic propagation effects that can thereby be observed. We also survey some applications of slow and fast light within the fields of quantum electronics and photonics.

## 2. Fundamentals of slow and fast light

Slow and fast light refer to the group velocity of a light wave. The group velocity is the velocity most closely related to the velocity at which the peak of a light pulse moves through an optical dispersive material (Milonni, 2005), and is given by the standard result

$$v_g = \frac{c}{n_g}, \qquad n_g = n + \omega \frac{dn}{d\omega} \tag{1}$$

where $n$ is the refractive (phase) index and $\omega$ is the angular frequency of the carrier wave of the light field. One refers to light as being slow light for $v_g << c$, fast light for for $v_g > c$, and backwards light for $v_g < 0$ or $v_g$ is negative. Extreme values of the group velocity invariably rely on the dominance of the second contribution to the group index of Equation (1). This contribution of course results from the frequency dependence of the refractive index, and for this reason extreme values of the group velocity are usually associated with the resonant or near-resonant response of material systems.

According to this theory, slow light is expected in the wings of an absorption line and fast light is expected near line center, and the spatial dispersion, that is, the non-locality in space of the medium response, is another mechanism that can lead to slow light, as has been predicted (Kocharovskaya et al,2001) and observed (Strekalov et al, 2001). We catalogue the main methods to realize slow light in room temperature solid, namely slow light via stimulated Brillouin scattering(SBS), slow light via coherent population oscillations (CPO), tunable time delays based on group velocity dispersion or conversion/ dispersion(C/D), slow light in fiber Bragg gratings and so on. We will describe CPO and SBS slow light in more details.

## 3. Slow light via coherent population oscillations (CPO)

### 3.1 Introduction of CPO

The technique of coherent population oscillation(CPO) is also exploited to reduce the group velocity.The process of CPO allows the reduction of absorption and simultaneously provides a steep spectral variation of the refractive index which leads to a strong reduction of the optical group velocity,i.e.,slow light propagation.This process is easily achieved in a two-level system which interacts with a signal whose amplitude is periodically modulated.The population of the ground state of the medium will be induced to oscillate at the modulation frequency. This oscillation creates an arrow hole in the absorption spectrum, whose linewidth is proportional to the inverse of the relaxation lifetime of the excited level. CPO is highly insensitive to dephasing processes in contrast to what happens in other schema such as EIT, where the width of the spectral hole burned in the absorption profile is proportional to the inverse of the dephasing time of the ground state. That makes CPO an appropriate technique to easily achieve slow light propagation in solid-state materials at room temperature.

### 3.2 Theoretical mode

Making use of this technology, we observe optical pulse delay and advancement propagation in an erbium-doped optical fiber. Compared to other solid material, erbium-doped optical fiber allows for long interaction lengths, which can be desirable in producing strong influence(Schwartz& Tan, 1967). We obtain the controllable pulse delay continuously from positive to negative by using a separate pump laser.

When pumped at 980nm, the erbium-doped fiber acts as a three-level molecular system. The relaxation time from the metastable state to the ground state is much greater than the one from the excited state to the metastable state. The energy levels and pumping scheme that we employed to observe slow and fast light in erbium-doped fiber is shown in Fig 1.

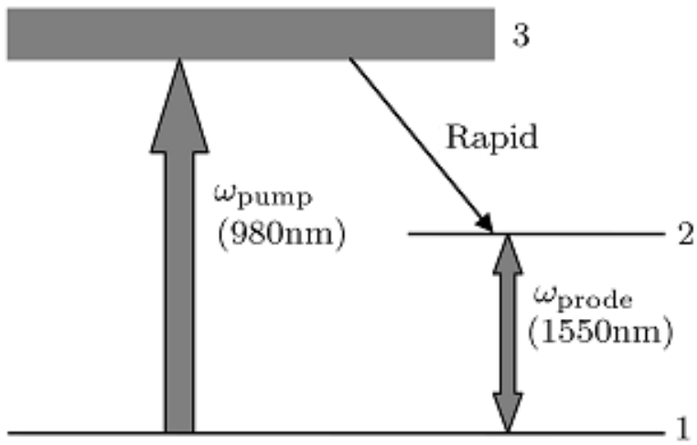


Fig. 1. The energy levels and pumping scheme we employed to observe slow and fast light in erbium-doped fiber.

The relaxation time from the excited state associated with the signal frequency to the ground state is much greater than the one from the excited state associated with the pump frequency to the excited state associated with the signal frequency. The population of upper excited level is approximately equal to zero, which indicates $n_1 + n_2 = \rho$. The population density of the ground state will accord with the rate equation(Novak & Gieske, 2002)

$$\frac{\partial n_1}{\partial t} = -R_{13}n_1 - W_{12}n_1 + W_{21}(\rho - n_1) + \frac{\rho - n_1}{T_1}, \tag{2}$$

where $W$ denotes transition rates associated with signal and $R$ presents transition rates associated with pump. $T_1$ is the lifetime of the excited state and $\rho$ is the erbium ion density. The transition rates are also functions of $t$ and $z$, as well as being proportional to the pump and signal powers. According to the equations for the transition rates and neglecting the losses through the fiber, we have

$$\frac{\partial}{\partial t}N_1 = I_p(L,t) - I_p(0,t) + I_s(L,t) - I_s(0,t) + \frac{N_0 - N_1}{T_1}. \tag{3}$$

If we modulate the signal(~1550nm) intensity as

$$I(0,t) = I_s^0(0)\left(1 + \mu_s \cos\delta t\right). \tag{4}$$

here, $I_s^0(0)$ is the average input power at the input ($Z$=0) and $I_s^0(0)\mu_s = I_m(0)$ is the modulation amplitude. A single intensity-modulated beam contains only a carrier wave (to act as the pump) and two sidebands (to act as probes) on the output spectrum, which induce population oscillation. The population of the ground state is given by

$$N_1(t) = N_1^0\left[1 + \xi \cdot \cos\left(\delta t + \phi\right)\right], \tag{5}$$

where $N_1^0$ is the mean (un-modulated) steady-state population. We next find the steady-state solution to Eq. (3). Finally, We can determine the expression of the delay of the optical signal

$$\Delta t = \frac{1}{\delta \times 2\pi} \arctan\left( \frac{\delta}{\frac{\delta^2{}_{eff} + \delta^2}{\eta} - \delta_{eff}} \right). \tag{6}$$

### 3.3 Experimental results

The signal optical field from a distributed feedback laser diode operating at 1550nm through the attenuator is divided into two parts: one part of laser (98%) goes through an erbium-doped optical fiber and then to an InGaAs photodetector with 10MHz bandwidth. The other part of laser output signal (2%) is sent directly to an identical photodetector to be used as reference.Transmitted signals are received by photodetectors, and sent into a digital oscillograph for recording. Then the comparison between the reference signal and the EDOF signal is made in a computer (Sargent,1978, Boyd & Gauthier, 2005). The group velocity in fibers can be inferred. In the experiments, the injection current of the laser is sinusoidally modulated by a function generator. We use single mode, $Al_2SiO_5$-glass-based erbium-doped optical fibers at several ions density. The experimental setup is shown in Fig.2.

The absorption coefficient $\alpha$ and the emission coefficient $\beta$ are related to their cross sections respectively and shown by the following

$$\alpha_s = \Gamma_s \sigma_{12} \rho \quad \alpha_p = \Gamma_p \sigma_{13} \rho \quad \beta_s = \Gamma_s \sigma_{21} \rho \,. \tag{7}$$

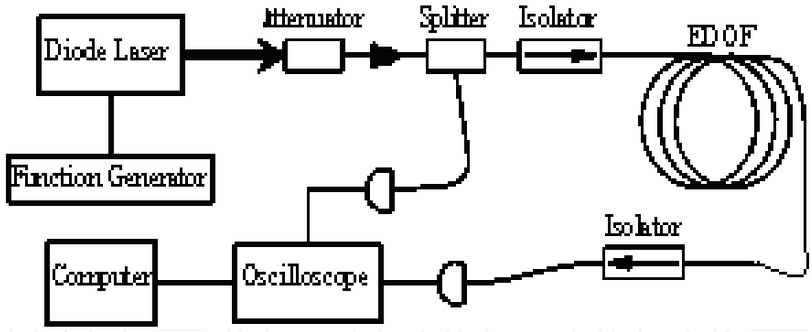


Fig. 2. The experimental setup used to observe slow light in an erbium-doped optical fiber.

Parameters used for the calculation are $\alpha_s$ =31.71 dB/m, $\alpha_p$ =42.3dB/m, $\beta_s$ =47.665 dB/m, $T_1$ = 10.5 ms, $L$=2m, and $\rho$ =6.3×$10^{25}$. Our experimental results are obtained through use of modulation techniques such that the optical field contains only a carrier wave (to act as the pump)and two sidebands (to act as probes). Because the decay time is so long (about 10.5ms), this oscillation will only occur if the beat frequency ($\delta$) between the pump and probe beams is small so that $\delta T_1 \sim 1$.When this condition is fulfilled, the pump wave can efficiently scatter off the temporally modulated ground state population into the probe wave, resulting in reduced absorption of the probe wave. We consider the Kramers-Kronig relations, which show that a narrow hole in an absorption spectrum will produce strong normal dispersion. Fig.3 illustrates the results of our experiments.

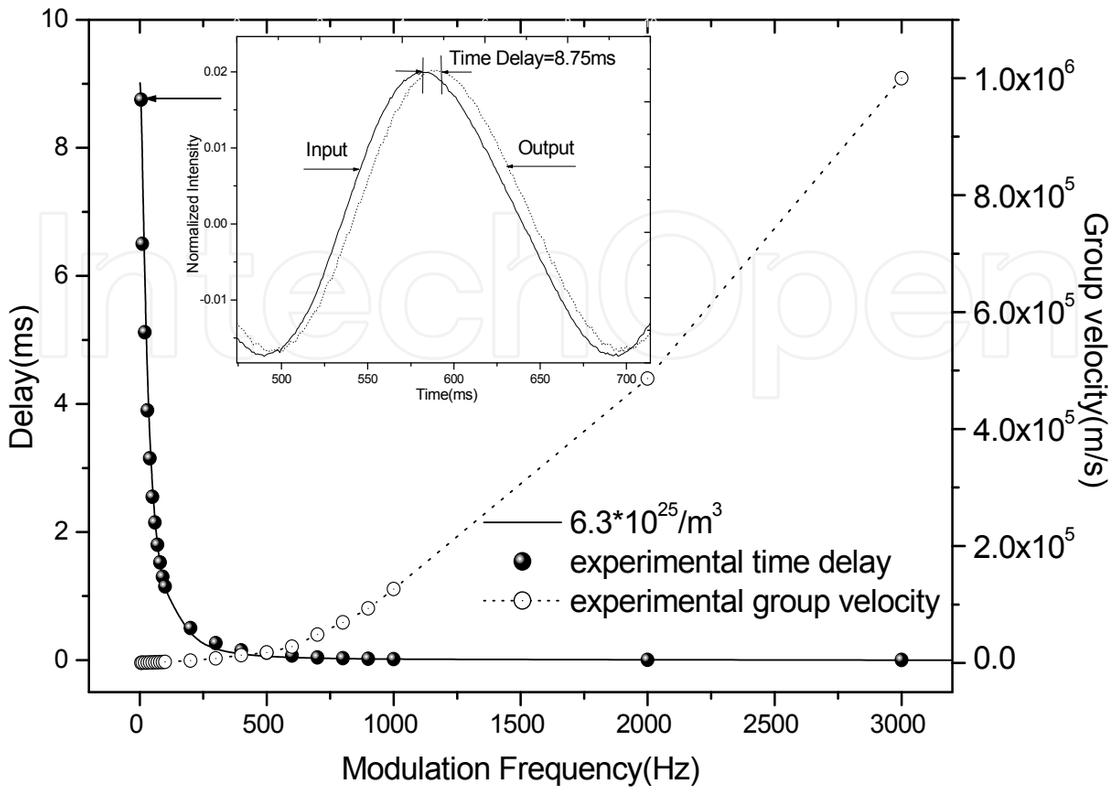


Fig. 3. Observed time delay as a function of the modulation frequency for input power of 1.85mW. The solid line is the theoretical fit to the experimental data. The open circles represent the measured group velocity. The inset shows the normalized 5Hz input (solid line) and output (dashed line) signal. The signal is delayed 8.75ms corresponding to a group velocity as low as 228.57m/s.

In Fig.3, we show the measured delay in an optical fiber with erbium ion density of $6.3\times10^{25}m^{-3}$ and compare it with the numerical solution of Eq.(6) for input power of 1.85mW. We observe the largest delay, 8.75ms, which corresponds in the inset of Fig.3. The inferred group velocity is as low as 228.57m/s. A maximum fractional delay of 0.129 is observed at the modulation frequency of 60Hz. Fig.3 shows the delay as a function of modulation frequency in the low frequency region.

## 4. Slow light via stimulated Brillouin scattering (SBS)

### 4.1 Introduction

Slow light based on stimulated Brillouin scattering (SBS) in optical fibers has attracted much more interests for its potential application in optical buffering, data synchronization, optical memories and optical signal processing. Compared with previously demonstrated slow-light techniques (Gehring et al, 2008, Zhu et al, 2007), such as electromagnetically induced transparency (EIT) (Hau et al, 1999) and coherent population oscillations (CPO) (Bigelow et al, 2003), it has a lot of advantages, for instance, the simple, flexible and easy-to-handle SBS can be realized in room temperature; the optical fiber components based on it can easily integrated with the existing telecommunications infrastructure; the slow-light resonance can

be tunable within the optical communications wavelength windows; the use of optical fiber allows for a relaxed pump-power requirement owning to long interaction length, small effective mode area and so on.

However, the SBS-induced group index change is always so small in standard single mode fiber and dispersion shift fibers (DSFs) (Song et al, 2005) to delay the time very little. In order to explore suitable optical fibers served as slow light generation with much efficiency, some special optical fibers, such as chalcogenide fiber (Abedin,2005, Song et al, 2006), tellurite fiber (Abedin,2006), bismuth fiber (Jauregui et al, 2006) and so on, have been extensively studied, these kinds of optical fiber are usually with large gain coefficient and low loss coefficient. Though long pulse delay can be obtained using cascaded fiber segments joined by unidirectional optical attenuators to overcome pump depletion (gain saturation) and amplified spontaneous Brillouin emission (ASBE), it's always accompanied with serious pulse distortion (Song et al, 2005). So gain tailoring is used in pulse distortion management to keep a balance between time delay and pulse distortion (Stenner et al, 2007). To overcome the narrow band spectral resonance of SBS which limits the maximum data rate of the optical system, a simple and inexpensive pump spectral broadening technique is used in broadening the SBS slow light bandwidth (Herraez et al, 2006), which paves the way towards real applications based on SBS slow light.

Numerical studies of SBS slow light focusing on different pulse parameters were also studied (Kalosha et al, 2006), which provide an insight into the SBS slow light process, but we can't learn a lot about how the optical fiber structures and Brillouin gain parameters influence on the SBS process, the time delay and the pulse shape. In this section, the SBS model in optical fiber is described and the three coupled SBS equations are solved by the method of finite difference with prediction-correction, the effects of gain coefficient, gain bandwidth and effective mode area on time delay and pulse broadening are demonstrated. Considering the injected stokes pulse shape, the influence of its sharpness, magnitude and duration on delay time and pulse broadening factor was observed mainly, and its reason was analyzed. These results provide base for designing optical buffer, time delay line or other optical components based on the SBS slow light technologies.

### 4.2 Theory foundation and numerical model

The process of SBS is the interaction of two counter-propagating waves, a strong pump wave and a weak Stokes wave. If a particular frequency relation is satisfied

$$v_{pump} = v_{Stokes} + v_B , \tag{8}$$

Where $v_{pump}$ and $v_{Stokes}$ are the frequency of pump wave and stocks wave respectively, $v_B$ is the Brillouin frequency. Then an acoustic wave is generated which scatters photons from the pump to the Stokes wave and the interference of these two optical waves in turn stimulates the process. From a practical point of view, the process of SBS can be viewed as a narrowband amplification process, in which a continuous-wave pump produces a narrowband gain in a spectral region around $v_{pump} - v_B$. In this paper, the Stokes pulse is set on the SBS gain line center to achieve the maximum delay.

For simply describing the SBS process, assume: (1) Transverse field variations are neglected, Stokes and pump fields are assumed to vary with time t and space z only. (2) The slowly varying envelope approximation (SVEA) SBS model is used, i.e., the field amplitudes are

assumed to vary slowly in time and space as compared with their temporal and spatial frequencies. (3) The initial (t=0) phonon field is zero and the Stokes output grows from an injected Stokes field at z=0. (4) The frequency difference between the pump and Stokes wave is set to the Brillouin shift of the fiber, i.e., the Stokes pulse is on the SBS line center.

Considering a Brillouin amplifier where the pump wave counter-propagates through the fiber with respect to the Stokes pulse, the SBS process can be described by one-dimensional coupled wave equations involving a backward pump wave (−z direction), a forward Stokes wave (+z direction), and a backward acoustic wave. Under the slowly varying envelope approximation (SVEA) and neglecting the transverse field variations, the equations are written as follows (Damzen et al,2003)

$$-\frac{\partial A_p}{\partial z}+\frac{n}{c}\frac{\partial A_p}{\partial t}=-\frac{\alpha}{2}A_p+ig_2A_sQ\,, \tag{9}$$

$$\frac{\partial A_s}{\partial z}+\frac{n}{c}\frac{\partial A_s}{\partial t}=-\frac{\alpha}{2}A_s+ig_2A_pQ^*\,, \tag{10}$$

$$\frac{\partial Q}{\partial t}+\frac{\Gamma_B}{2}Q=ig_1A_pA_s^*\,, \tag{11}$$

where $A_p$, $A_s$, and $Q$ are the amplitudes of the pump wave, the Stokes wave, and the acoustic wave, respectively; $n$ is the group refractive index when SBS is absent; $\alpha$ is the loss coefficient of the fiber; $\Gamma_B/2\pi$ is the bandwidth (FWHM) of the Brillouin gain; $g_1$ is the coupled coefficient between the pump wave and the Stokes wave, $g_2$ is the coupled coefficient between the pump (Stokes) wave and the acoustic wave, $g_0=4g_1g_2/\Gamma_B$ is the peak value of the Brillouin gain coefficient.

According to the small signal steady state theory of stimulated Brillouin scattering, the pump power $P_{critical}$ required to reach Brillouin threshold in a single pass scheme is related to the Brillouin gain coefficient $g_0$ by the following equation:

$$g_0(P_{critical}/A_{eff})L_{eff}\cong 21\,, \tag{12}$$

where $P_{critical}$ is the power corresponding to the Brillouin threshold, $L_{eff}$ is the effective length defined as $L_{eff}=\alpha^{-1}[1-\exp(-\alpha L)]$, from Eq.(12) we can obtain the threshold pump intensity

$$I_{critical}=P_{critical}/A_{eff}\cong 21/(g_0L_{eff})\,. \tag{13}$$

Once reaching the threshold pump intensity, a large part of the pump power is transferred to the Stokes wave, resulting in the generation of Stokes wave at the output depletes the pump seriously and leads to serious Stokes pulse distortion. In our simulations, we consider the pump intensity is near the Brillouin threshold and obtain the Stokes gain around 16 using the previous parameters, here the Stokes gain is defined as:

$$Gain=\log\left(\frac{P_{out}}{P_{in}}\right), \tag{14}$$

where $P_{out}$ and $P_{in}$ are the output and input of the Stokes power, respectively.
Let us assume that pump wave is continuous wave and stokes field is sufficiently weak. The group index is the function of frequency described as follow(Zhu et al, 2005)

$$n(\omega_s) = n_g + \frac{cg_B I_p}{\Gamma_B} \frac{1 - 4\delta\omega^2 / {\Gamma_B}^2}{(1 + 4\delta\omega^2 / {\Gamma_B}^2)^2} \tag{15}$$

where $I_p$ is the optical intensity of pump wave; $\delta\omega$ is the margin between the angular frequency of stokes pulse and the center angular frequency of the gain bandwidth; $g_B = \frac{{\gamma_e}^2 {\omega_p}^2}{n_g v_B c^3 \rho_0 \Gamma_B}$ is the line-center gain factor which is associated with the material physical properties, $v_B$ is the velocity of acoustic wave.
Delay time $T_d$ is defined to describe the difference of the arrival time when the output stokes pulse reach its maximum between when SBS occurs and doesn't occurs, $T_{rd} = T_d / T$ to describe the relative delay time with T which is the FWHM of the injected stokes pulse. According to the weak signal theory, delay time and B are given by (Velchev et al, 1999)

$$T_d = G / \Gamma_B \tag{16}$$

$$B = \sqrt{1 + \frac{16 \ln 2}{T^2 {\Gamma_B}^2} G} \tag{17}$$

where $G = g_B I_p L$ is the weak signal gain parameter; L is the fiber length. For the purpose of indicating how much the pump wave energy contributes to the stokes wave energy, we define real gain as

$$G_r = \log(P_{\text{out}} / P_{\text{in}}) \tag{18}$$

where $P_{out}$ and $P_{in}$ are power of the output and input stokes wave, respectively.
We assume that injected stokes pulse is super-Gaussion shaped

$$U(t) = \exp\left( -\frac{1}{2} \left( \frac{t}{T_0} \right)^{2m} \right) \tag{19}$$

where t is the time of pulse transmission, U(t) is normalized amplitude, $T_0$ is the half width of pulse (at 1/e-intensity point). The parameter m controls the degree of edge sharpness (for m=1, it is Gaussion-shaped; for m>1, it is super-gaussion-shaped, and the degree of edge sharpness is increased with m). For different m, pulse with same FWHM can be written as

$$U(t) = \exp\left( -2^{2m} (\ln 2) \left( \frac{t}{T} \right)^{2m} \right) \tag{20}$$

Furthermore, we define average intensity of normalized super-Gaussion pulse with FWHM of T as

$$\bar{I}_s = \frac{1}{T}\int_{-T/2}^{T/2} \left(U(t)\right)^2 dt = \frac{1}{T}\int_{-T/2}^{T/2} \left(\exp\left(-2^{2m}(\ln 2)\frac{t^{2m}}{T^{2m}}\right)\right)^2 dt \tag{21}$$

In our numerical processing, applying the slowly-varying envelope approximation (SVEA) for both pump and stokes fields, firstly, we obtained the values of $\rho$ at some time by solving the Eq.(11) with Fourier transformation and inverse Fourier transformation. Secondly, we transform the Eqs (9-10) into single variable partial differential equations by using characteristics. Finally, applying the value of $\rho$ we obtained to the single variable partial differential equations, we can calculate the values of $E_p$ and $E_s$ at next time by using the fourth-order Runge-Kutta formula. And we set these results as the initialization value to achieve the value of $\rho$ at next time. Repeating above steps, we can achieve the output stokes pulse at anytime.

### 4.3 Numerical simulation results

In order to study the situation where the pump is depleted, we solve the Eqs. (9)-(11) numerically using the method of implicit finite difference with prediction-correction to determine how gain coefficient, gain bandwidth and effective mode area influence SBS slow light.

In our simulation, the parameters are considered from the common single-mode fiber, and select: fiber length L=25m, pump wavelength $\lambda$ =1550nm, group refractive index n=1.45, effect mode area $A_{eff}$ =50 $\mu m^2$, loss coefficient $\alpha$ =0.2dB/km, gain bandwidth (FWHM) $\Gamma_B / 2\pi$ =40MHz, gain coefficient $g_0 = 5\times10^{-11}$ m/W. We assume the pump wave is CW and the Stokes wave is Gaussian shaped with the peak power of 0.1 $\mu W$ and the FWHM pulse width of 120ns (its FWHM bandwidth in frequency domain is around 3.7MHz which is much smaller than that of SBS gain bandwidth we use).

#### 4.3.1 Influence of gain coefficient on time delay and pulse broadening

The curves of the pulse delay and pulse broadening factor as a function of the gain with different gain coefficient $g_0$ were shown in Fig.4. It can be seen from Fig.4(a) that the time delay increases linearly with Stokes gain when the gain is small (≤10), that's because the pump isn't completely affected when the gain is small. For larger gain, pump depletion becomes more and more seriously, the time delay increases slowly with gain and reaches its maximum before decreasing with gain. At the same time, for larger gain coefficient, the time delay decreases with increasing gain more quickly and even leads to pulse advancement which can be explained by gain saturation. It can also be seen that the smaller gain coefficient reaches the gain saturation at a larger gain and the maximum time delay is accordingly larger, the gain saturation limits the maximum time delay for a Stokes pulse at a given input power.

The pulse broadening factor for different gain coefficients as a function of gain was shown in Fig.4(b). It shows that the pulse broadening factor is also increasing linearly with gain when the small signal regime holds. As the gain further increases, the pulse broadening factor increases slowly with gain and then gradually decreases to less than 1, it means that the pulse become more and more narrower, the pulse with larger gain coefficient narrows more seriously than the smaller one. The time delay is always accompanied with pulse distortion, the Stokes pulse broadens a little in the small signal regime but can narrow

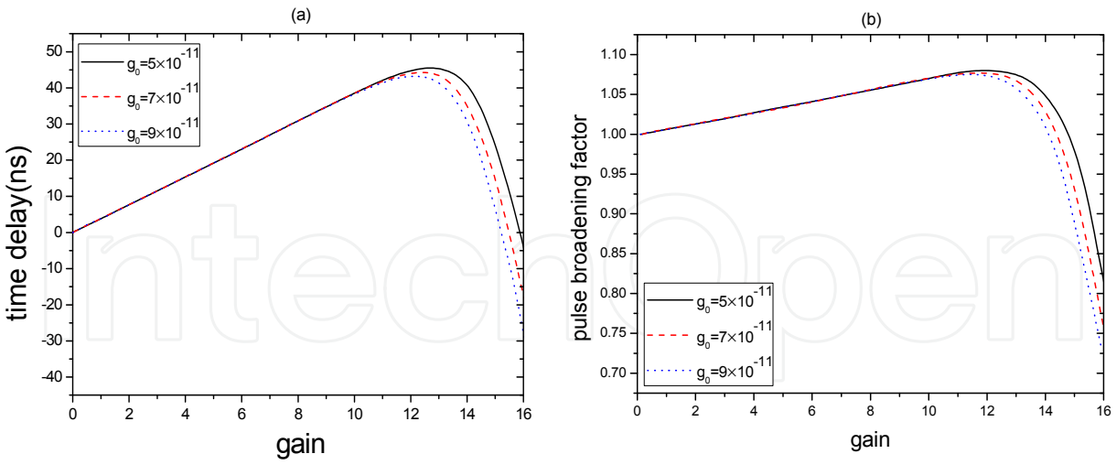


Fig. 4. (a) Time delay and (b) pulse broadening as a function of gain with different gain coefficients.

largely in the gain saturation regime. Fig.5 shows the normalized output pulse shapes with the gain coefficient $g_0 = 5\times10^{-11}$ m/W at gain=0, 12, and 17, respectively. The output Stokes pulse with a maximum time delay ~45 ns at gain=12 with a little distortion while the output Stokes pulse is advanced by 42.9 ns at gain=17 but is distorted substantially.

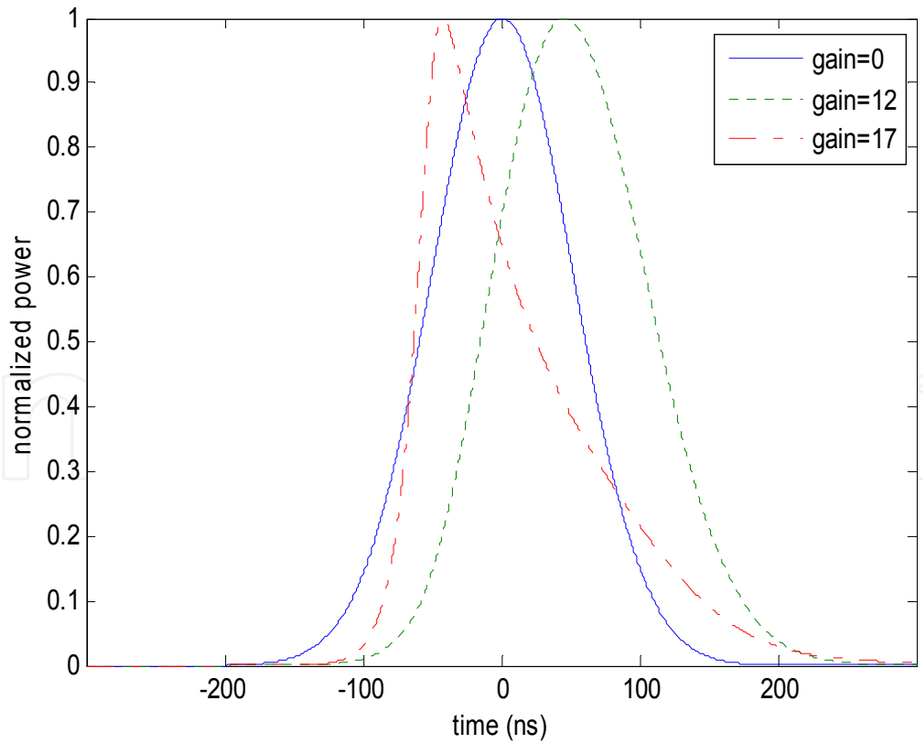


Fig. 5. Normalized output Stokes pulse at gain=0, 12, 17 with the gain coefficient $g_0 = 5\times10^{-11}$ m/W.

Next, we consider the time delay and pulse broadening factor varying with the gain coefficient at a given pump peak power 0.125W shown in Fig.6. From Fig.6(a) we can see that the time delay increases with the increasing gain coefficient in a linear fashion. Fig.6(b) shows that the pulse broadening factor also increases with the increasing gain coefficient. Note that the maximum gain parameter is 6.25 at the gain coefficient $g_0 = 1 \times 10^{-10}$ m/W, which satisfies the small signal condition.

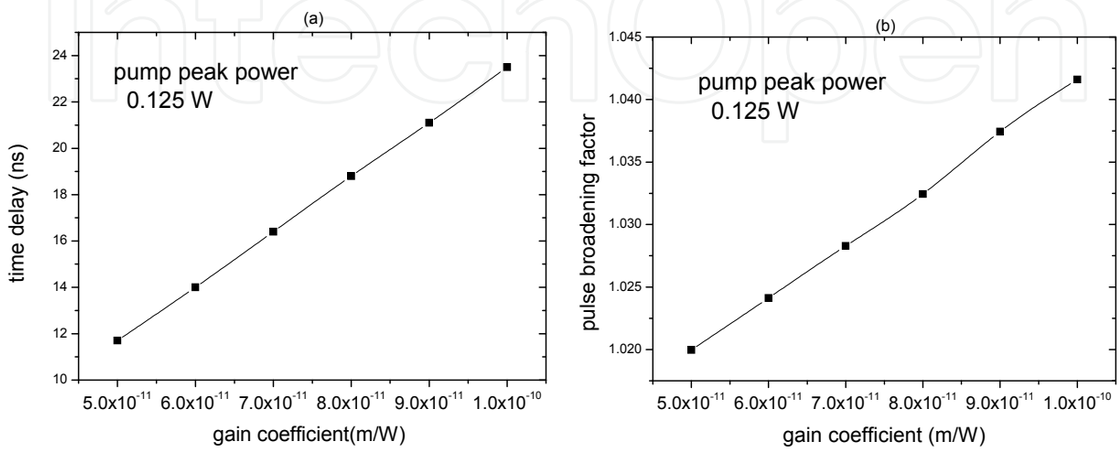


Fig. 6. (a) Time delay and (b) pulse broadening as a function of gain coefficient at a given pump power.

### 4.3.2 Influence of gain bandwidth on time delay and pulse broadening

Fig.7(a) shows the time delay as a function of gain with different gain bandwidths. The time delay increases with the gain linearly when the gain is small, but for smaller gain bandwidth, the time delay increases with the gain more quickly and reaches the saturation at a larger gain, the maximum time delay is accordingly larger. Once reaching the gain saturation, the time delay also decreases more quickly for smaller gain bandwidth.

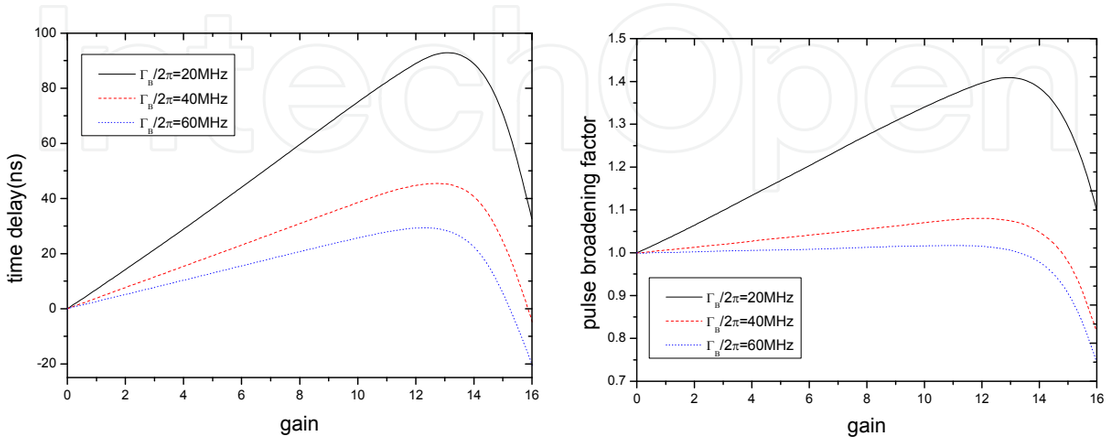


Fig. 7. (a) Time delay and (b) pulse broadening as a function of gain with different gain bandwidths.

The pulse broadening factor as a function of gain with different gain bandwidths was shown in Fig.7(b). It can be seen that the pulse broadening factor increases with the gain before gain saturation and then it decreases with the increasing gain which is similar with time delay versus gain in Fig.7(a). The smaller the gain bandwidth is, the more quickly the broadening factor increases with the gain in the small signal regime and decreases with the gain in the gain saturation. It indicates that the pulse with smaller gain bandwidth always obtains the longer time delay but at the cost of much larger pulse broadening.
We also calculated the time delay and pulse broadening factor as a function of gain bandwidth at a given pump peak power 0.125W. As we can see in Fig.8, both the time delay and pulse broadening factor decrease with the increasing gain bandwidth and keep an inverse proportion to it. The maximum gain parameter is 6.25, which is also in the small signal regime for these different gain bandwidths.

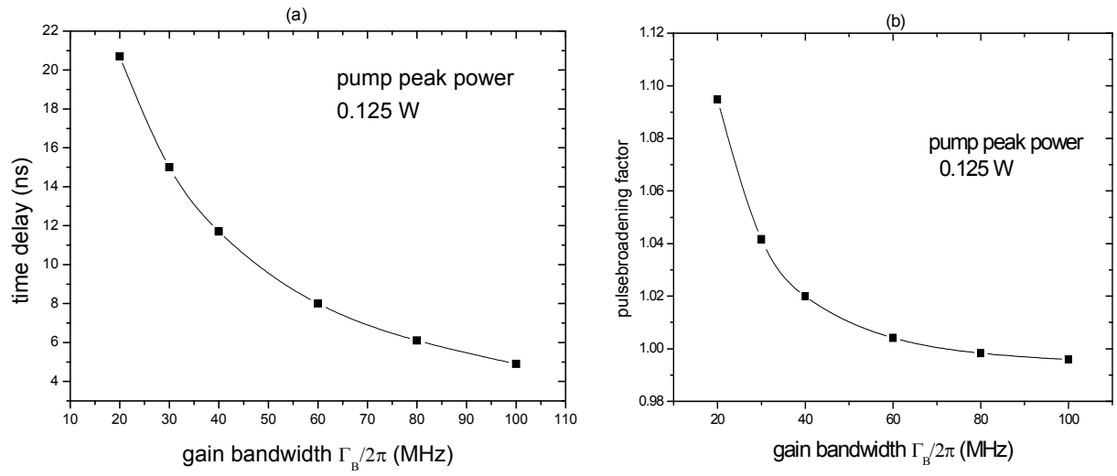


Fig. 8. (a) Time delay and (b) pulse broadening as a function of gain bandwidth at a given pump power.

#### 4.3.3 Influence of effective mode area on time delay and pulse broadening

For the pulse with same peak power, it has a larger intensity for the smaller effective mode area, which increases its intensity in the other way, so it can also influence the gain saturation obviously. As can be seen from Fig.9(a), in the small signal regime, the time delay still increases with the gain linearly for different effective mode areas, the pulse with smaller effective mode area reaches the gain saturation at a smaller gain, and the maximum time delay is accordingly smaller. Once reaching the gain saturation, the pulse with smaller effective mode area also decrease more quickly than the others.
Fig.9(b) shows the pulse broadening factor versus gain, the pulse broadening factor increases linearly with the increasing gain in the small signal regime, which is the same as the time delay versus gain. As has been said before, the pulse with larger effective mode area reaches the gain saturation at a larger gain and its maximum pulse broadening factor is accordingly larger. In the gain saturation regime, the pulse with smaller effective mode area narrows more seriously than the others at a fixed gain. We can even see that the pulse broadening factor begins to increase for the gain around 16.

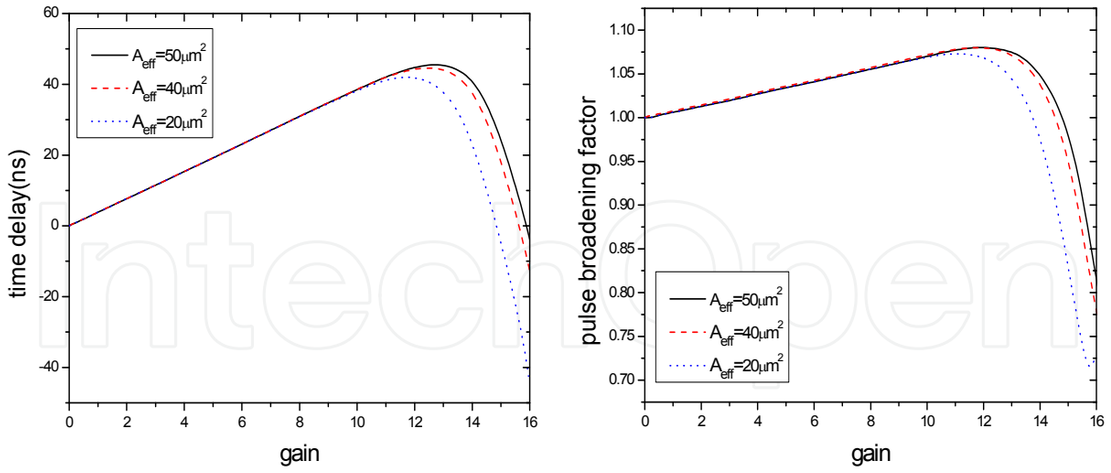


Fig. 9. (a) Time delay and (b) pulse broadening as a function of gain with different effective mode areas.

We also investigate the time delay and pulse broadening factor as a function of effective mode area at a given pump power 0.125W. It can be seen from Fig.10, both the time delay and pulse broadening factor decrease with the increasing effective mode area and keep an inverse proportion to it. As previously mentioned, we also make sure that the corresponding gain parameter is within the small signal regime for these different effective mode areas.

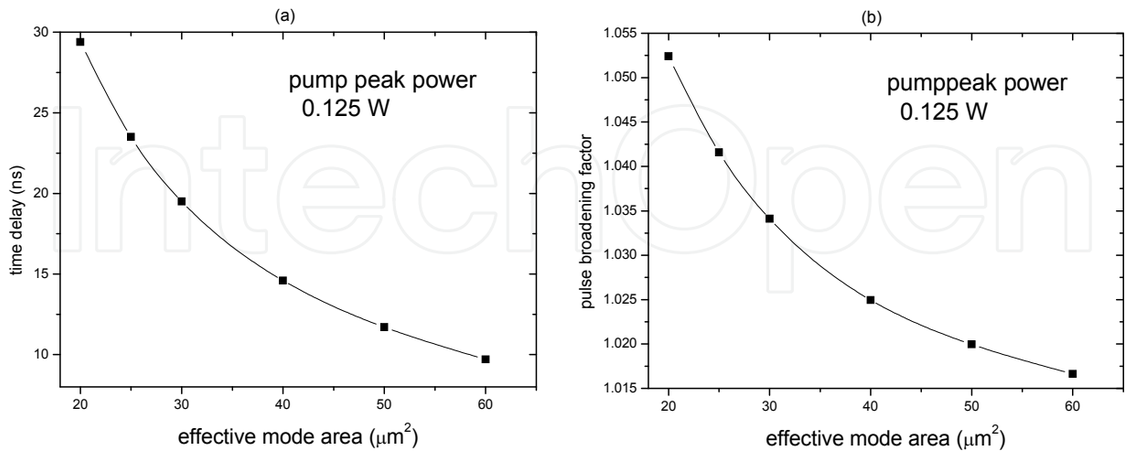


Fig. 10. (a) Time delay and (b) pulse broadening as a function of effective mode area at a given pump power.

#### 4.3.4 The influence of stokes pulse with different m on SBS slow light

We first consider the pulse time delay and pulse broadening factor as a function of parameter real gain for super-Gaussion-shaped pulse with different m, which is indicated in Fig.11. In this case, T=120ns, $P_{in} = 0.1\mu W$ . Fig.11 (a) shows that with the increase of $G_r$ , $T_d$ increases accordingly and reaches its maximum. Then it decreases with further increasing $G_r$ , even becomes negative. Comparing with different m, we can see that maximum $G_r$ and the time when maximum $G_r$ obtains decrease with m because when m changes from 0.5 to 3, $\overline{Is}$ is equal to 0.5410, 0.6805, 0.7559 and 0.8705, respectively, i.e., for the same duration and apex, the super-Gaussion-shaped pulse with higher m is easier to reach gain saturation. And $T_d$ when $T_d$ reaches its maximum will decrease, which leads to the reducing of maximum $T_d$ .

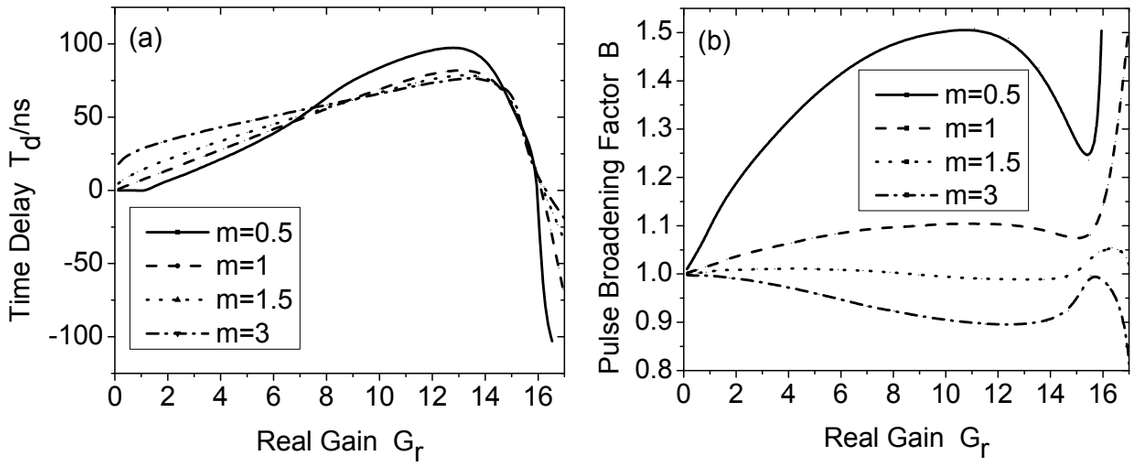


Fig. 11. Parameters of output stokes pulse versus real gain for different parameter m. a) Time delay $T_d$ versus real gain; b) Pulse broadening factor B versus real gain.

We observe an advantageous phenomenon for practical applications. When m=1.5, pulse broadening factor B is close to 1. While m=3, B decreases with increasing $G_r$ and reaches its peak value at gain=13. Then it increase with $G_r$ and reaches its maximum at $G_r$ =15.5, it decrease with further increasing $G_r$ . The reason why B has the rule can be explained well by Fig.12. Considering SBS process and no SBS process, respectively, for three different m, the normalized output stokes pulses at $G_r$ =5 and $G_r$ =13 are shown in Fig.12, where t is the time axis. It is indicated from Fig.12 (a) that with increasing m the leading edge and the trailing edge of super-Gaussion-shaped pulse become steeper and steeper in time domain. So they will become broader and broader in the frequency domain. Considering equation (2), we can conclude that the difference among the speeds of points at the leading edge will increase and the leading edge will be compressed more. Moreover, the increasing m leads to the increasing energy of pulse with same peak value. And most energy of pump wave is

depleted in the leading edge of stokes pulse, the trailing edge only can get less energy from pump wave, the broadening of the trailing edge of stokes pulse is limited. All of this can contribute to decreasing B and result in B is almost close to 1 before stokes pulse is near saturation. When $G_r$ increases to saturation gain step by step, the trailing edge gets more and more energy, resulting in broadening of the trailing, i.e., B will increase, like shown in Fig.12(b). When $G_r$ go on increasing, it is out of the range of weak signal, the output stokes pulse is distortion seriously.

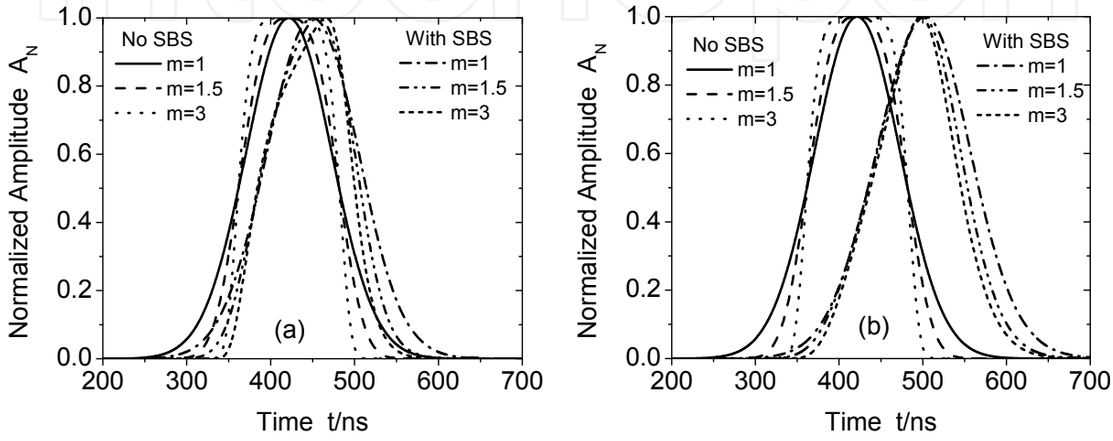


Fig. 12. Output stokes pulse for different real gain. a) $G_r$ =5; b) $G_r$ =13.

#### 4.3.5 The influence of stokes pulse with different power and FWHM on SBS slow light

Based on the result of above that when m=1.5 B is very close to 1, the next numerical simulation will select different power and duration of super-Gaussion pulse with m=1.5 as the injected stokes pulse. Fig.13 shows that delay and B as a function of parameter $G_r$ for super-Gaussion-shaped pulse with different power. It can be seen form Fig.13 (a) that maximum $T_d$ and $G_r$ needed for obtaining maximum $T_d$ increase with injected power. And before entering gain-saturation regime $T_d$ is equal to each other. The reason is in the condition of weak signal delay is in direct proportion to gain approximately. As we can see from Fig.13(b) that when $G_r$ is smaller than saturation gain, B is close to 1 and B of the pulse which has the largest power will reach the peak shown in Fig.11(b) firstly with increasing $G_r$. The peak value becomes lager and larger, which correspond to high power pulse is easy to enter saturation regime.

Fig.14 shows that $T_{rd}$ and B as a function of parameter $G_r$ for super-Gaussion-shaped pulse with different T. The power of injected stokes pulse is 0.1 $\mu W$ and other parameter is the same like above. It is indicated that smaller duration pulse can obtain lager relative delay. The $G_r$ needed for obtaining maximum $T_{rd}$ becomes lager and larger with the decreasing T. The reason is for same peak value the smaller duration pulse contains less energy. Then when it enters gain-saturation regime it need more energy and higher saturation gain results in higher $T_{rd}$. The changing rule of pulse broadening factor of the pulse which duration is less than 120ns is different from the one which duration is 120ns, however, it is the same with the one when injected stokes pulse is Gaussion-shaped. The main reason is the energy

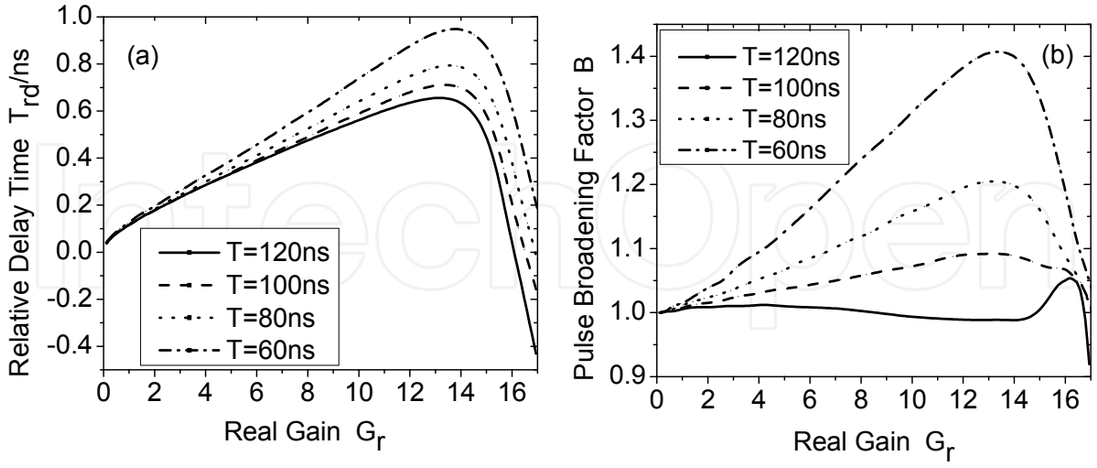


Fig. 13. Parameters of output stokes pulse versus real gain for different power. a)Time delay $T_d$ versus real gain; b) Pulse broadening factor B versus real gain.

which pulse contains decrease with the decreasing duration for same peak value. The energy getting from pump wave decreases, too. So the tailing edge of stokes pulse can obtain more energy than the one when T=120ns, resulting in the tailing edge broaden widely. This counteracts the compression corresponding to the steep leading edge. It can be predicted that increasing m can make the leading edge steeper and can decrease B. Our numerical result proved it. For the pulse with T=60ns, B at maximum $T_{rd}$ decreases from 1.406 to 1.295 when m is changed from 1.5 to 5.

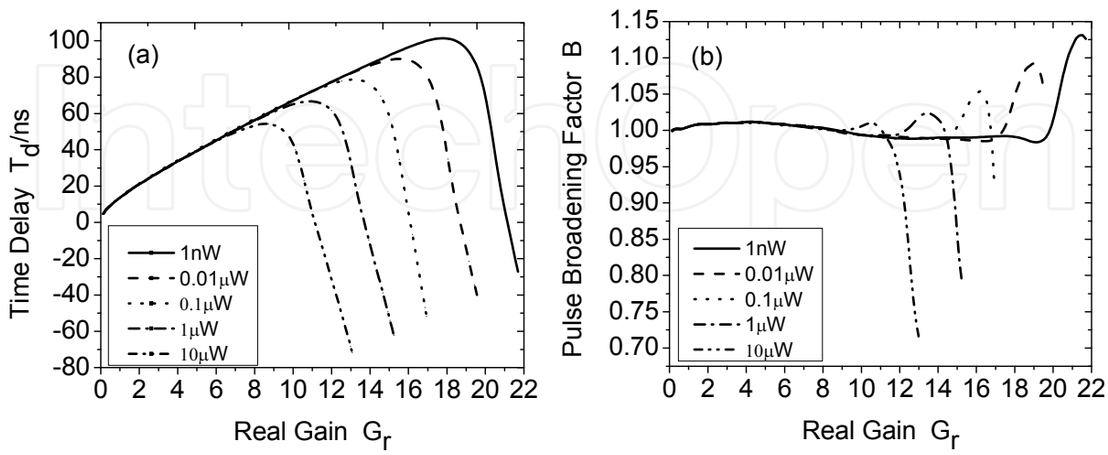


Fig. 14. Parameters of output stokes pulse versus real gain for different duration. a) Relative time delay $T_{rd}$ versus real gain; b) Pulse broadening factor B versus real gain.

## 5. Conclusion

We make a numerical study of the SBS slow light in optical fibers, and consider the influences of gain coefficient, gain bandwidth and effective mode area on time delay and pulse broadening. In the small signal regime, we find that the time delay and the pulse broadening factor increase with the increasing gain, but for pulse with the smaller gain bandwidth has a larger slope than the others. In the gain saturation regime, the pulse with larger gain coefficient, smaller gain bandwidth, smaller effective mode area begins to decrease more quickly in the gain range of 0~16. For the gain larger than 16, the pulse advancement becomes more obviously and the distortion also becomes more seriously, which may render the delay useless. We also investigate the time delay and pulse broadening factor vary with the increasing gain coefficient, gain bandwidth and effective mode area at a given pump power whose gain parameter is in the small signal regime, and find that the time delay and pulse broadening factor are proportional to the gain coefficient, whereas inversely proportional to the gain bandwidth and the effective mode area.

According to the above numerical calculation and theory analysis, we find that decreasing the power and duration of injected stokes pulse induces increasing delay time and pulse broadening factor; using super-Gaussion-shaped pulse as the injected stokes pulse can contribute evidently to decreasing pulse broadening factor in low frequency. Selecting pretty m can get perfect delay time and pulse broadening factor. Though this adjusting effect will become weaker for a shorter pulse, this reform still takes advantage of decreasing the error rate of all-optical-buffer.

## 6. Acknowledgment

This work was supported by the National Natural Science Foundation of China (Grant No. 61167005), the Provincial Natural Science Foundation of Gansu Province (Grant No. 1010RJZA036), the Provincial Natural Science Foundation of Guangdong Province (Grant No. 1104511700030049 48) and Dongguan Science and Technology Program (Grant No.2008108101002).

## 7. References

Boyd R.W. and Gauthier D. J.(2009), Controlling the Velocity of Light Pulses, *Science*, Vol.326,No.5956,pp.1074-1077, ISSN 0036-8075.

Stenner M. D, Gauthier D. J, Neifeld M. A(2003). The speed of information in a 'fast-light' optical medium, *Nature*, Vol. 425, pp. 695-698.ISSN0028-0836.

Gehring G. M, Schweinsberg A., BarsC. i, Kostinski N., Boyd R. W.(2006) Observation of Backward Pulse Propagation Through a Medium with a Negative Group Velocity, *Science*, Vol.312,No.5775,pp.895-897, ISSN 0036-8075.

Brillouin L(1960), *Wave Propagation and Group Velocity* ,Academic Press, New York.

Faxvog F. R, Chow C. N. Y, Bieber T., and Carruthers J. A(1970). Measured Pulse Velocity Greater Than *c* in a Neon Absorption Cell, *Appl. Phys. Lett.*, Vol.17, No.5, pp.192-193,ISSN0003-6951.

Hau L. V., Harris S. E., Dutton Z. et al(1999). Light speed reduction to 17 metres per second in an ultracold atomic gas. *Nature*, Vol.397, pp.594–598, ISSN0028-0836.

Philips D. F., Fleischhauer A., Mair A. et al(2001). Storage of light in atomic vapor. *Phys. Rev. Lett.*, Vol. 86,No.5,pp.783–786. ISSN1079-7114.

Bigelow M. S., Lepeshkin N. N., Boyd R. W(2003). Superluminal and slow light propagation in a room-temperature solid. *Science*, Vol.301,No.5630,pp.200–202, ISSN 0036-8075.

Milonni P. W(2005), *Fast Light, Slow Light, and Left-Handed Light*, Institute of Physics Publishing, Bristol, UK.

Kocharovskaya, O.; Rostovtsev, Y.; Scully, M.O(2001). Stopping light via hot atoms, *Phys. Rev. Lett*. Vol. 86,No.4,pp. 628-631, ISSN1079-7114.

Strekalov, D.; Matsko, A.B.; Yu, N.; Maleki, L.J. J(2004). Influence of inhomogeneous broadening on group velocity in coherently pumped atomic vapour, *Mod. Opt.* Vol.51, No.16,pp.2571-2578, ISSN0950-0340.

Schwartz S.E, Tan T.Y(1967). Wave Interactions in Saturable Absorbers. *Appl. Phys. Lett.* Vol. 10,No.1,pp.4~7, ISSN0003-6951.

Hillman L.W., Boyd R.W., Krasinski J., and Stroud C.R(1983). Observation of a Spectral Hole Due to Population Oscillations in a Homogeneously Broadened Optical Absorption Line. *Opt. Commun.* Vol. 45,No.6,pp. 416~419, ISSN0030-4018.

Bigelow M. S., Lepeshkin N. N., and Boyd R. W(2003). Observation of Ultraslow Light Propagation in a Ruby Crystal at Room Temperature. *Phys. Rev. Lett.* Vol.90, No.11,pp. 113903, ISSN1079-7114.

Boyd R.W(1992). *Nonlinear Optics* , Academic Press, San Diego.

A. Schweinsberg, N. N. Lepeshkin, M. S. Bigelow, R.W.Boyd, and S.Jarabo. Observation of Superluminal and Slow light Propagation in Erbium-Doped Optical Fiber. Europhys. Lett. 2006,73(2):218-224

Shin H., Schweinsberg A., Gehring G., Schwertz K., Chang H. J., and Boyd R. W(2007). Reducing Pulse Distortion in Fast-Light Pulse Propagation through an Erbium-Doped Fiber Amplifier. *Opt. Lett.*, Vol.32,No.8,pp.906-908,ISSN0146-9592.

Song K. Y., Herráez M. G., and Thévenaz L.(2005). Long Optically Controlled Delays in Optical Fibers. *Opt. Lett.*, Vol.30,No.14,pp.1782-1784, ISSN0146-9592.

Novak S., Gieske R(2002). Analytic Model for Gain Modulation in EDFAs. *J Lightwave Technol*., Vol.20,No.6,pp.975-985,ISSN0733-8724.

Sargent III M(1978). Spectroscopic techniques based on Lamb's laser theory. *Phys. Rep.*,Vol. 43,No.5,pp. 223-265,ISSN0370-1573.

Boyd,R. W, Gauthier D. J, Gacta A.L, and Willner A.E(2005). Maximum Time Delay Achievable on Propagation through a Slow-light Medium. *Phys. Rev. A.*, Vol. 71,No.2,pp.023801-1-023801-4, ISSN1094-1622.

Gehring G. M., Boyd R. W.,. Gaeta A.L., Gauthier D. J. and Willner A. E(2008). Fiber-Based Slow-Light Technologies, *Journal of Lightwave Technology*, Nol.26,No.23,pp. 3752-3762 , ISSN0733-8724 .

Zhu Z., Gauthier D. J., Boyd R.W(2007). Stored Light in an Optical Fiber via Stimulated Brillouin Scattering, *Science*, Vol.318,No.5857,pp.1748-1750, ISSN 0036-8075.

Song K. Y., Herraez M. G., and Thevenaz L(2005). Observation of pulse delaying and advancement in optical fibers using stimulated Brillouin scattering, *Opt. Express*, Vol.13,No.1,pp.82-88 , eISSN1094-4087.

Abedin K. S.(2005), Observation of strong stimulated Brillouin scattering in single-mode As2Se3 chalcogenide fiber, *Opt. Express*, Vol.13,No.25,pp.10266-10271,eISSN1094-4087.

Song K. Y, Abedin K. S, Hotate K., Herraez M. G and Thevenaz L(2006), Highly efficient Brillouin slow and fast light using As2Se3 chalcogenide fiber, *Opt. Express*, Vol.14,No.13, pp.5860–5865, eISSN1094-4087.

Abedin K. S(2006), Stimulated Brillouin scattering in single-mode tellurite glass fiber, *Opt. Express*, Vol.14,No.24, pp.11766–11772, eISSN1094-4087.

Jauregui C., Ono H., Petropoulos P. and Richardson D. J(2006), Four-fold reduction in the speed of light at practical power levels using Brillouin scattering in a 2-m bismuth-oxide fiber, in *Proc. of Conference on Optical Fiber Communication (OFC 2006)*, Paper PDP2 .

Stenner M. D., Neifeld M. A., Zhu Z., Dawes A. M. C. and Gauthier D. J(2005). Distortion management in slow-light pulse delay, *Opt. Express,* Vol.13, No.25, pp. 9995-10002 , eISSN1094-4087.

Schneider T., Henker R., Lauterbach K. U., and Junker M(2007). Comparison of delay enhancement mechanisms for SBS-based slow light systems, *Opt. Express*, Vol.15,No.15),pp.9606-9613, eISSN1094-4087.

Schneider T., Henker R., Lauterbach K. U., and Junker M(2008). Distortion reduction in Slow Light systems based on stimulated Brillouin scattering, *Opt. Express*, Vol.16,No.11,pp. 8280-8285, eISSN1094-4087.

Herraez M. G, Song K. Y., and Thévenaz L. (2006), Arbitrary-bandwidth Brillouin slow light in optical fibers, *Opt. Express* , Vol.14, No.4, pp.1395-1400, eISSN1094-4087.

Zhu Z., Dawes A. Gauthier M. C., D. J., Zhang L., and Willner A. E. (2006), 12-GHz-Bandwidth SBS Slow Light in Optical Fibers, in *Proc. of OFC 2006*, paper PD1.

Song K. Y., Hotate K. (2007), 25 GHz bandwidth Brillouin slow light in optical fibers, *Opt. Lett.* , Vol.32 , No.3, pp.217-219, ISSN0146-9592.

Zhu Z., Gauthier D. J., and et al(2005), Numerical study of all-optical slow-light delays via stimulated Brillouin scattering in an optical fiber, *J. Opt. Soc. Am. B*, Vol.22 , No.11, pp.2378-2384, ISSN0740-3224.

Kalosha V. P., Chen L, and Bao X. Y(2006), Slow and fast light via SBS in optical fibers for short pulses and broadband pump, *Opt. Express,* Vol.14, No.26, pp. 12693-12703, eISSN1094-4087

Damzen M. J., Vlad V. I., Babin,V. and Mocofanescu A(2003), *Stimulated Brillouin Scattering: Fundamentals and Applications*, IOP Publishing, ISBN0 7503 0870 2.

Dane C. B., Neuman W. A. and Hackel L. A. (1994), High-energy SBS pulse compression, *IEEE J. Quantum Electro*, Vol.30, No.8, pp.1907-1915, ISSN0018-9197.

Zhu Z., Gauthier D. J., Okawachi Y, *et al*(2005). Numerical study of all-optical slow-light delays via stimulated Brillouin scattering in an optical fiber, *J. Opt. Soc. Am. B,* Vol.22, No.11, pp. 2378- 2384, ISSN0740-3224.

Velchev I., Neshev D., Hogervorst W., and Ubachs W(1999). Pulse compression to the subphonon lifetime region by half-cycle gain in transient stimulated Brillouin scattering. *IEEE J. Quantum Electron*, Vol.35, No.12, pp.1812-1816, ISSN0018-9197.


**Recent Progress in Optical Fiber Research**

Edited by Dr Moh. Yasin

ISBN 978-953-307-823-6

Hard cover, 450 pages

**Publisher** InTech

**Published online** 25, January, 2012

**Published in print edition** January, 2012

This book presents a comprehensive account of the recent progress in optical fiber research. It consists of four sections with 20 chapters covering the topics of nonlinear and polarisation effects in optical fibers, photonic crystal fibers and new applications for optical fibers. Section 1 reviews nonlinear effects in optical fibers in terms of theoretical analysis, experiments and applications. Section 2 presents polarization mode dispersion, chromatic dispersion and polarization dependent losses in optical fibers, fiber birefringence effects and spun fibers. Section 3 and 4 cover the topics of photonic crystal fibers and a new trend of optical fiber applications. Edited by three scientists with wide knowledge and experience in the field of fiber optics and photonics, the book brings together leading academics and practitioners in a comprehensive and incisive treatment of the subject. This is an essential point of reference for researchers working and teaching in optical fiber technologies, and for industrial users who need to be aware of current developments in optical fiber research areas.



**InTech Europe**
University Campus STeP Ri
Slavka Krautzeka 83/A
51000 Rijeka, Croatia
Phone: +385 (51) 770 447
Fax: +385 (51) 686 166
www.intechopen.com

**InTech China**
Unit 405, Office Block, Hotel Equatorial Shanghai
No.65, Yan An Road (West), Shanghai, 200040, China
中国上海市延安西路65号上海国际贵都大饭店办公楼405单元
Phone: +86-21-62489820
Fax: +86-21-62489821

IntechOpen